Available online at www.sciencedirect.com
ScienceDirect
Trans. Nonferrous Met. Soc. China 25(2015) 437−443
Transactions of Nonferrous Metals Society of China
www.tnmsc.cn

Effect of standard heat treatment on microstructure and properties of borided Inconel 718

De-wei DENG, Chun-guang WANG, Qian-qian LIU, Ting-ting NIU

School of Material Science and Engineering, Dalian University of Technology, Dalian 116024, China

Received 31 March 2014; accepted 14 July 2014

Abstract: Boronizing was applied to Inconel 718. In order to obtain the optimal combination of strength and ductility, the borided Inconel 718 was subjected to standard heat treatment. This consists of solution treatment and then a two-step aging treatment. The borided layer is composed of the compound layer and the boron diffusion zone. Because of the superior hardness of borides, the borided Inconel 718 exhibits a significant reduction in its wear rate and relatively low coefficient of friction (COF) compared with the unborided Inconel 718. The standard heat treatment efficiently promotes the diffusion of boron into the interior of the material and the generation of new borides (Fe_2B, CrB). The borided layer with standard heat treatment shows much better wear resistance due to the thicker borided layer (313.76 μm).

Key words: boronizing; Inconel 718; standard heat treatment; wear resistance; corrosion resistance

1 Introduction

Inconel 718 is a precipitation-hardenable nickel-based superalloy, strengthened primarily by ordered face centred cubic (FCC) γ'-Ni_3 (Al,Ti) and ordered body centred tetragonal (BCT) γ''-Ni_3Nb. Based on its high strength, outstanding weldability, favourable corrosion resistance and excellent microstructure stability at elevated temperature (650 °C), Inconel 718 is widely used in gas turbines, rocket motors, spacecraft, nuclear reactors and pumps [1−3]. In spite of these excellent properties, Inconel 718 has unsatisfactory wear characteristics [4]. Thus, it is desirable to improve the wear resistance of Inconel 718 without adversely affecting its corrosion resistance. Thermochemical technologies are regarded as good methods for this demanding objective. Compared with ferrous materials and stainless steels, the application of thermochemical technologies to superalloys has received little attention. Only few studies have been reported and most of them have focused on plasma nitriding of Ni-based superalloys [4−6]. It was reported that the thicknesses of the nitrided layers were no more than 15 μm. Such alloys are well known to be extremely difficult to be nitrided [5], but it is possible to get thicker layers by applying boronizing to Ni-based superalloys, because boron can easily form borides such as Ni_3B, Ni_2B, Ni_4B_3 and NiB_2 with nickel [7]. Some researchers have reported thicker borided layers of superalloys borided by different boronizing methods [8−10]. However, the effects of solution and aging treatments, which were standard for these superalloys to obtain the optimal combination of strength and ductility in industry [11], were not considered for those borided superalloys described in previous studies.

Boronizing, as a thermochemical technology in which boron atoms diffuse into the surface to form borides with the basic material, has been developed in industry since 1970s [12]. There are many favourable properties of the borided layers, such as high hardness and sawtooth shape morphology, giving rise to good wear resistance and excellent adhesion strength [13−15]. The boriding process may be in the gas, liquid or solid state. The paste-boriding process, as a conventional boronizing technique in the solid state, can be carried out in an inert atmosphere as well as in a powder-filler (Al_2O_3/charcoal). This is convenient for obtaining a borided layer on specified positions of large-sized workpieces [16].

In this work, a borided layer was applied to Inconel 718 using the paste-boriding process, which should

Foundation item: Projects (2011CB013402, 201303002, 2014028002) supported by the National Basic Research Program of China
Corresponding author: De-wei DENG; Tel: +86-13998509875; E-mail:deng@dlut.edu.cn
DOI: 10.1016/S1003-6326(15)63621-4

provide a significant combination of high hardness, excellent wear resistance and good corrosion resistance. The microstructure, wear resistance and corrosion resistance of the borided layer were studied. Furthermore, the effects of the solution and aging treatments on the borided layer were investigated. Experimental samples were studied by optical microscopy, X-ray diffraction (XRD), micro-hardness testing, micro-tribometer and electron probe micro analyzer (EPMA).

2 Experimental

Samples of Inconel 718 (10 mm × 10 mm × 40 mm) were abraded by SiC abrasive papers and polished with 1.5 μm diamond as the final step. Inconel 718 was produced by vacuum induction melting (VIM) and vacuum arc remelting (VAR) technologies. The nominal elemental composition of Inconel 718 is given in Table 1.

Table 1 Nominal elemental composition of Inconel 718 (mass fraction, %)

Fe	Cr	Nb+Ta	Mo	Ti
18.53	18.47	5.18	3.09	0.94
Al	Si	C	Mn	Ni
0.48	0.08	0.032	0.01	Balance

The paste-boriding process was applied to the samples under a pure nitrogen atmosphere. In this process, a boron source (B_4C), activators (KBF_4, $NaBF_4$ and rare earth oxides) and inert materials (SiC, Al_2O_3 and Al) were thoroughly mixed to form the paste-boriding mixture. Boronizing was carried out in an electrical resistance furnace at 980 °C for 10 h, followed by cooling in air. The standard heat treatment (solution treated at 1050 °C for 1 h with air cooling to room temperature and a two-step aging treatment consisting of 720 °C for 8 h with furnace cooling at rate of 50 °C /h to 620 °C and then holding at 620 °C for 8 h followed by air cooling to room temperature, as shown in Fig. 1) was performed to investigate its effect on the microstructure and properties of the borided samples.

A Leica MEF-4A optical microscope was used to measure the depth of the borided layer. The samples were mechanically polished and etched with an aqueous solution consisting of potassium ferrocyanide (1 g/mL), potassium ferricyanide (10 g/mL) and potassium hydroxide (30 g/mL).

X-ray diffraction experiments were performed using a D/Max-2500PC X-ray diffractometer. The X-ray source was Cu K_α (λ=0.154060 nm) and the measurements were carried out over the 2θ range from 20° to 90° at a scanning rate of 1 (°)/min.

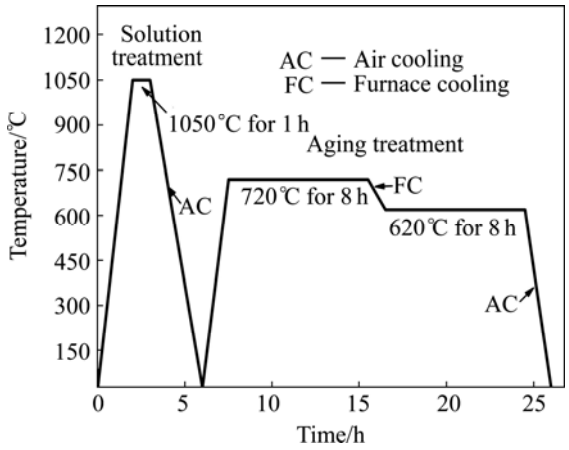

Fig. 1 Standard heat treatment for borided Inconel 718

The distribution of boron in the borided layer was measured using a Shimadzu 1600 electron probe micro analyzer (EPMA) with the method of linear scan analysis. It was also used to study the morphology of the borided layer.

The micro-hardness profile of the borided layer was measured along linear arrays from the surface to the interior, using a DMH-2LS Knoop micro-hardness instrument with a load of 0.49 N. The reported values were the average of at least three measured values.

Reciprocating ball-on-flat wear experiments were conducted on the samples to characterize the tribological behaviour by a CETR UMT-2 micro-tribometer. The coupled parts of the wear experiments were GCr15 steel balls, 5 mm in diameter. The experiments were performed in the laboratory at a sliding velocity of 1 mm/s for a reciprocating distance of 5 mm under a 10 N load. The coefficient of friction (COF) was measured continuously during the experiment. The wear rates of the samples were determined by measuring the width of the worn track via optical microscopy. At least five readings were taken for each worn track.

The corrosion behaviour was assessed in 5% H_2SO_4 (mass fraction) aqueous solution exposed to the laboratory environment for 20 h. The corrosion resistance was determined by the gravimetric method. After the corrosion experiment, the corrosion products were removed by mechanical and chemical procedures to measure the mass loss.

An ideal procedure should remove only the corrosion products and not result in the removal of any base metal. To determine the mass loss of the base metal when removing corrosion products, the replicated uncorroded control samples must be cleaned by the same procedure used for the test samples. By weighing the control sample before and after cleaning, the extent of metal loss from the cleaning can be utilized to correct the corrosion mass loss.

The average corrosion rate, v (g/(m^2·h^1)), was calculated from the gravimetric data using the formula:

$$v=(m_0-m_1-m_2)/(A\cdot t) \quad (1)$$

where m_0 is the mass of the sample prior to the corrosion experiment (g), m_1 is the mass of sample after cleaning (g), m_2 is the mass loss of the uncorroded control sample resulting from cleaning (g), A is the area of the sample (m^2), and t is the time of exposure (h).

The corrosion ratio, B (mm/a), was determined by

$$B=K\cdot v/\rho \quad (2)$$

where K=8.76 (a constant) and ρ is the density of the sample (g/cm^3).

3 Results and discussion

3.1 Microstructure

Figure 2 shows the cross-sectional optical micrograph of Inconel 718 borided at 980 °C for 10 h (the borided Inconel 718). Three regions are identified in the cross-sections: the compound layer (Region *A*), the boron diffusion zone (Region *B*) and the interior (Region *C*). Since they are different from the sawtooth shape morphology of the borided carbon steels, the borided layers in this work are flatter [7,17]. The thickness of the compound layer is 104.88 μm, which is much thicker than that of the nitrided layers (no more than 15 μm) recorded in the previous works [4−6]. The thickness of the boron diffusion zone is 54.17 μm, which has a reticular morphology. It is obvious that the boron has mainly diffused along the grain boundary in the boron diffusion zone.

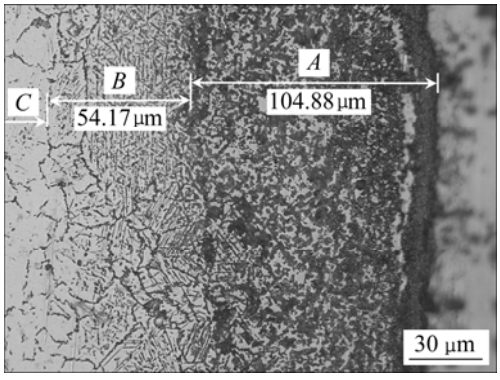

Fig. 2 Optical micrograph showing cross-sectional morphology of Inconel 718 borided at 980 °C for 10 h

Figure 3 shows the cross-sectional optical micrograph of Inconel 718 borided at 980 °C for 10 h followed by the standard heat treatment (the SA borided Inconel 718). The standard heat treatment has the effect of making the boron diffuse further into the substrate and also forming some new borides. The thicknesses of the compound layer (Region *A*) and the boron diffusion zone (Region *B*) are 313.76 μm and 133.12 μm, respectively. It is evident that the standard heat treatment can increase the depth of the borided layer.

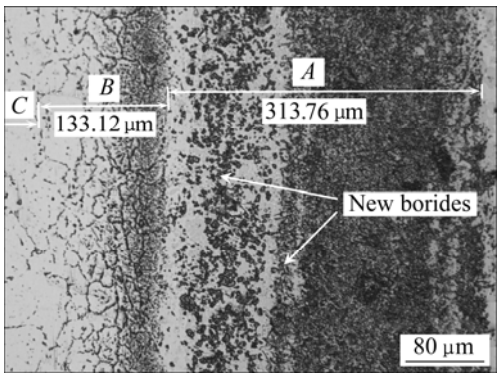

Fig. 3 Optical micrograph showing the cross-sectional morphology of Inconel 718 borided at 980 °C for 10 h followed by standard heat treatment

X-ray diffraction pattern also confirms the presence of Ni_2Si. However, the hardness of Ni_2Si is only HK 500 [9], which is much lower than that of the borided layer. The Ni_2Si layer is undesirable for the wear resistance of the borided Ni-based superalloys and should be removed in mechanical applications. In this work, the Ni_2Si layer is not taken into account and is removed before the performance tests.

3.2 Phase constitution of boriding layers

Because of the appearances of the mixed oxides and SiC in the paste-boriding mixture, the silicide Ni_2Si appears on the surface of the samples [9,18]. Figure 4 shows the X-ray diffraction patterns of the borided Inconel 718 and the SA borided Inconel 718. It is too complex to clearly identify the borides in the borided layer because of the existence of elements in Inconel 718, such as Fe, Nb and Cr, which can also be borided. The XRD analysis of the borided Inconel 718 shows that the interior consists of an FeNi alloy and the major borides in the compound layer (Region *A*) are Ni_2B and Ni_4B_3. The silicide Ni_2Si mentioned above is also recorded. The XRD analysis of the SA borided Inconel 718 clearly exhibits the existence of Fe_2B and CrB, which do not appear in the borided samples.

3.3 Boride formed after standard heat treatment

Figure 5 shows the EPMA linear scan profile of the SA borided Inconel 718. The new borides are also observed by EPMA and the element Fe is found to be aggregated in the region of new borides *A*. Figure 6 shows the SEM and optical micrographs of the new borides, which do not appear in the borided Inconel 718. The morphologies of the new borides are approximately

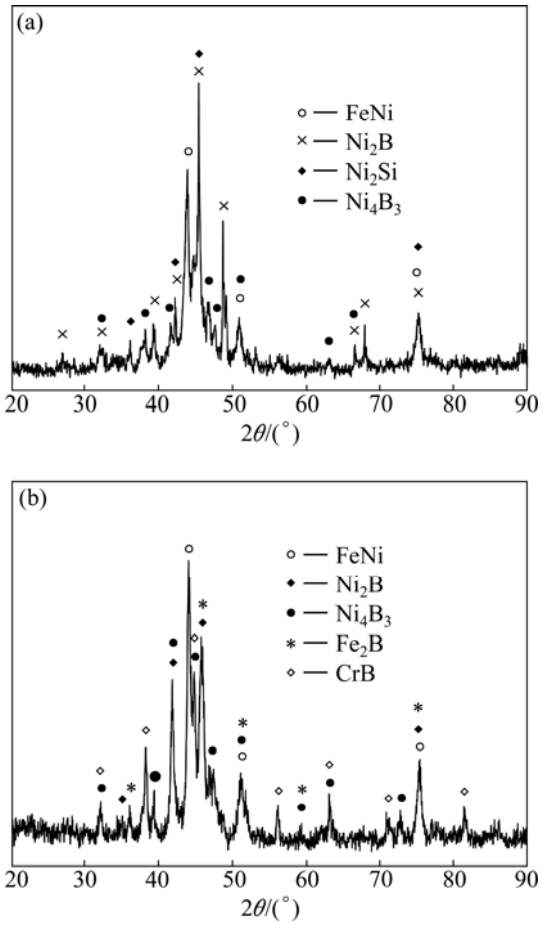

Fig. 4 X-ray diffraction patterns of borided Inconel 718 (a) and SA borided Inconel 718 (b) (The interior of samples consists of an FeNi alloy)

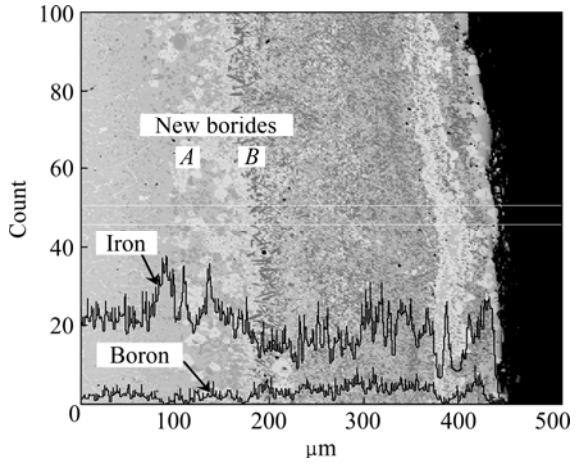

Fig. 5 EPMA linear scan profile of SA borided Inconel 718 (The boron distribution in the SA borided layer was homogeneous and iron (Fe) atoms were aggregated in the region of the new boride *A*)

rectangular and lath-shaped. It is interesting that the boride *A* exhibits rectangular morphology under the optical microscope, which is identical with the boride Fe_2B noted in previous works [13,19]. From the XRD analysis, the new borides are identified as Fe_2B and CrB. From the results of SEM-EDS, EMPA, XRD and optical microscopy, the new boride *A* (rectangular morphology) is Fe_2B and the new boride *B* (lath-shaped morphology) is CrB, as shown in Fig. 6.

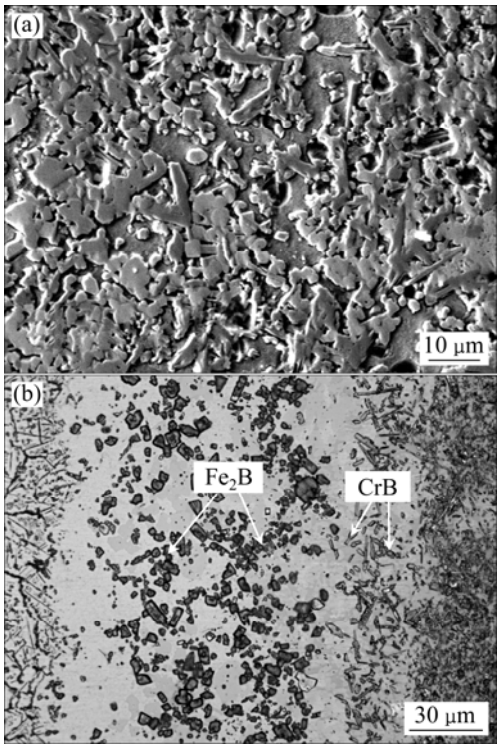

Fig. 6 SEM (a) and optical (b) micrographs showing morphologies of new borides

3.4 Boron content and hardness of borided layers

Figure 7 shows the micro-hardness and boron content of the borided Inconel 718 from the surface to the interior. The hardness of the borided layer is much higher than that of the interior due to the presence of hard borides [20]. The hardness is more than $HK_{0.05}$ 1600 on the surface, three times higher than that in the interior,

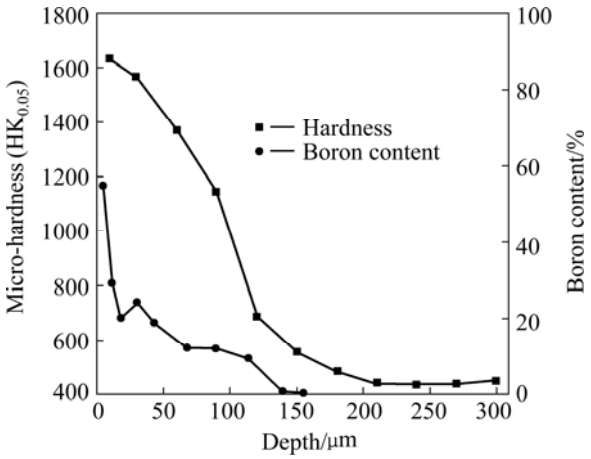

Fig. 7 Micro-hardness profile and boron content depth profile of borided Inconel 718

which is $HK_{0.05}$ 430.0. It is obvious that the boron content affects the hardness of the boriding layer, as shown in Fig. 7. In accordance with the boron content profile, the micro-hardness decreases with the depth from the surface to the interior.

Figure 8 shows the micro-hardness and boron content of the SA borided Inconel 718 from the surface to the interior. After the standard heat treatment, the highest micro-hardness is only $HK_{0.05}$ 1345.8. The decrease of the hardness can be correlated to the temper of the borided layer in the solution treatment. However, the depth of the higher hardness layer (more than $HK_{0.05}$ 1000) increases to 270 μm. This higher hardness layer will be quite valuable in industrial applications. The boron distribution in the SA borided layer is more homogeneous, ranging from 19.35%− 25.57%. Similarly, the hardness of the SA borided sample varies with the boron content.

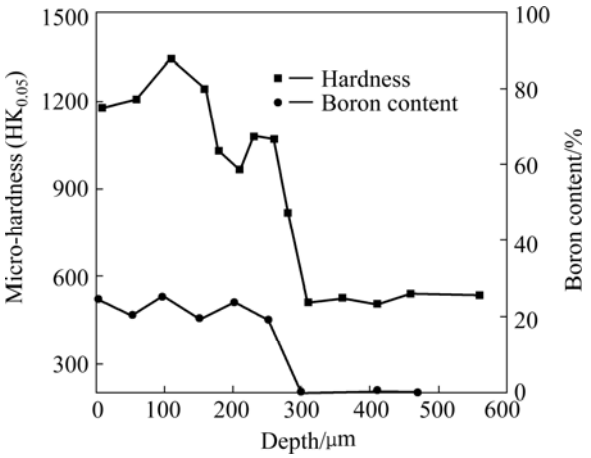

Fig. 8 Micro-hardness profile and boron content depth profile of SA borided Inconel 718

3.5 Tribological properties

The results of the wear test are shown in Figs. 9 and 10 as a function of the coefficient of friction (COF) and the wear rate, respectively. The COF of the unborided Inconel 718 against a GCr15 steel ball ranges from 0.7 to 0.8 in the present test conditions. Its wear rate is 1.782×10^{-3} mm^3/(N·m). The hardness of the unborided sample is only $HK_{0.05}$ 400−500, which is rather lower than that of the borided sample. The lower hardness would result in heavy plastic deformation under loads. The high COF and wear rate of the unborided Inconel 718 can be associated with the heavy plastic deformation, which takes place on the contact surface due to the destructive action of the coupled GCr15 steel ball [21].

The COF of the borided Inconel 718 gradually increases during the wear test, from 0.4 to 0.7. This gradual increase of the COF should owe to the sharp decrease of hardness with depth from surface to the

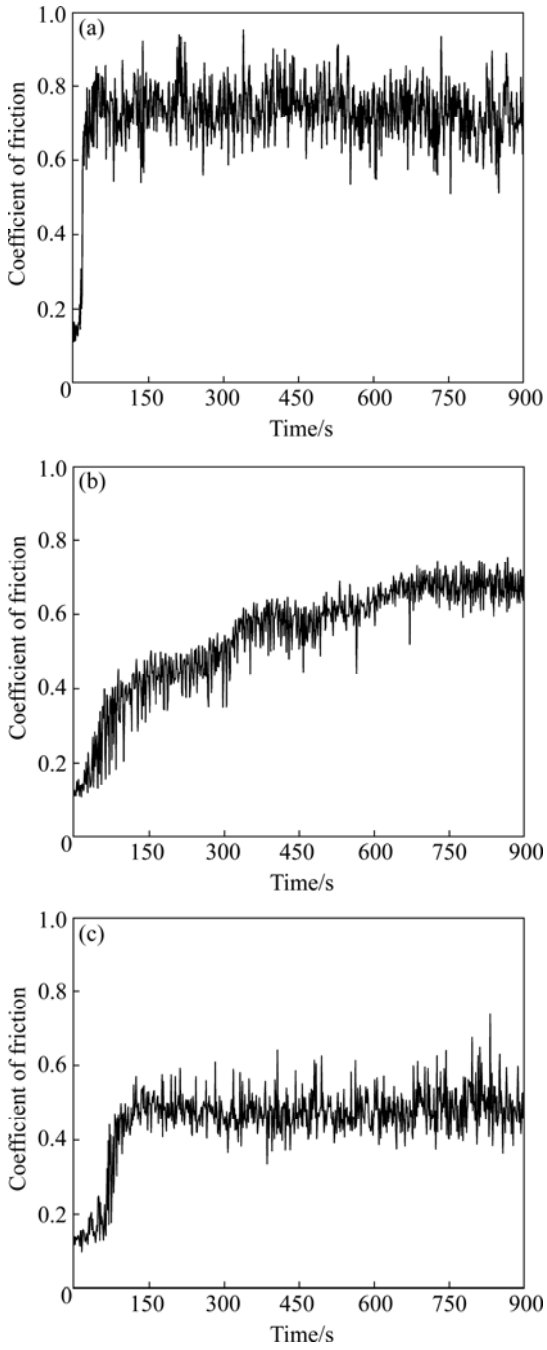

Fig. 9 Coefficient of friction of unborided Inconel 718 (a), borided Inconel 718 (b) and SA borided Inconel 718 (c)

interior. The wear rate of the borided sample is 0.126×10^{-3} mm^3/(N·m), which is only 7.07% that of the unborided sample. Obviously, the boronizing greatly enhances the wear resistance of Inconel 718 [22]. The abrupt reduction of the wear rate could be correlated with the superior hardness (more than $HK_{0.05}$ 1600) of the borided layer [21]. Because of the superior hardness, the contact between the borided sample and the GCr15 steel ball is less plastic and more elastic. During the wear test, the borided layer largely maintains elastic deformation

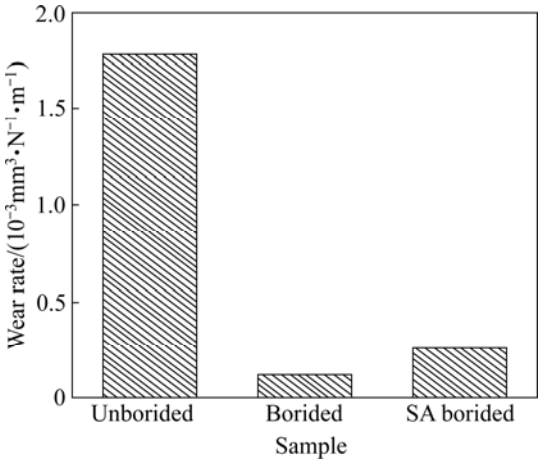

Fig. 10 Wear rates of Inconel 718 samples

under the reciprocating sliding of the GCr15 steel ball and only the limited plastic deformation is removed.

The SA borided Inconel 718 exhibits the lowest and most constant COF, ranging from 0.4 to 0.5, as well as a lower wear rate, 0.261×10^{-3} $mm^3/(N\cdot m)$. The standard heat treatment contributes to the lowest COF and the lower wear rate. The micro-hardness of the boride layer in the SA borided sample is more homogeneous, as shown in Fig. 8, and the hardness of the surface in contact with the GCr15 steel ball is relatively constant. There is no significant variation of COF during the wear test and the COF is much lower because of the especially hard surface. The wear rate of the SA borided sample is only 14.70% that of the unborided sample. Conclusively, the SA borided Inconel 718 exhibits excellent wear resistance in the wear experiment.

The wear results of the borided and SA borided Inconel 718 are consistent with other borided materials where a significant decrease in the COF and an abrupt reduction in the wear rate were observed [22]. UE et al [17] reported that the boriding method improved the friction and wear properties of 99.9% pure nickel [17].

3.6 Corrosion properties

Table 2 gives the corrosion results of the unborided, the borided and the SA borided Inconel 718. The unborided sample exhibits the most favourable corrosion resistance. The corrosion rates and the corrosion ratios of the borided sample and the SA borided sample are rather higher than those of the unborided sample. The boronizing treatments weakens the corrosion resistance of Inconel 718 to some extent. However, compared with the martensitic stainless steel FV520B, whose corrosion rate and corrosion ratio are respectively 7.2245 $g/(m^2\cdot h)$ and 8.0620 mm/a for identical corrosion conditions, the borided and SA borided Inconel 718 exhibits much better corrosion resistance.

Table 2 Corrosion results of Inconel 718 samples

Sample	Corrosion rate, $v/(g\cdot m^{-2}\cdot h^{-1})$	Corrosion ratio, $B/(mm\cdot a^{-1})$
Unborided	0.0195	0.0208
Borided	0.5869	0.6239
SA borided	1.2200	1.2969

4 Conclusions

1) Inconel 718 can be borided efficiently by the paste-boriding process. The borides in the borided layers, such as Ni_2B and Ni_4B_3, greatly enhance the hardness and the wear resistance of Inconel 718.

2) Application of the standard heat treatment to the borided Inconel 718 produces a positive result. The standard heat treatment promotes boron diffusion into the sample interior. The borided layer is found to show a two-fold increase in depth and two new borides (Fe_2B, CrB) appear alongside the boron diffusion zone. The SA borided Inconel 718 also exhibits excellent wear resistance.

3) Inconel 718 alloys which are borided and SA borided have sufficient corrosion resistance, better than some martensitic stainless steels.

References

[1] APPARAO G, KUMAR M, SRINIVAS M, SARMA D S. Effect of standard heat treatment on the microstructure and mechanical properties of hot isostatically pressed superalloy Inconel 718 [J]. Materials Science and Engineering A, 2003, 355(1−2): 114−125.

[2] PING D H, GU Y F, CUI C Y, HARADA H. Grain boundary segregation in a Ni−Fe based (alloy 718) superalloy [J]. Materials Science and Engineering A, 2007, 456(1−2): 99−102.

[3] RAHMAN M, SEAH W K H, TEO T T. The machinability of Inconel 718 [J]. Journal of Materials Processing Technology, 1997, 63(1−3): 199−204.

[4] SINGH V, MELETIS E I. Synthesis, characterization and properties of intensified plasma-assisted nitrided superalloy Inconel 718 [J]. Surface and Coatings Technology, 2006, 201(3−4): 1093−1101.

[5] SUN Y. Kinetics of layer growth during plasma nitriding of nickel based alloy Inconel 600 [J]. Journal of Alloys and Compounds, 2003, 351(1−2): 241−247.

[6] LEROY C, CZERWIEC T, GABET C, BELMONTE T, MICHEL H. Plasma assisted nitriding of Inconel 690 [J]. Surface and Coatings Technology, 2001, 142−144: 241−247.

[7] TORUN O. Boriding of nickel aluminide [J]. Surface and Coatings Technology, 2008, 202(15): 3549−3554.

[8] CURTIS D. Case hardening nickel alloys [J]. Materials and Design, 1993, 14(6): 349−350.

[9] MUHAMMAD W, HUSSAIN K, TAUQIR A, HAQ U L, AKHAN A Q. Evaluation of halide-activated pack boriding of inconel 722 [J]. Metallurgical and Materials Transactions A, 1999, 30(3): 670−675.

[10] CATALDO J, GALLIGANI F, HARRADEN D. Boride surface treatments [J]. Advanced Materials and Processes, 2000, 157(4): 35−38.

[11] REED R C. The superalloys: Fundamentals and applications [M]. New York: Cambridge University Press, 2006: 33−42.

[12] OZBEK I, BINDAL C. Mechanical properties of boronized AISI w4 steel [J]. Surface and Coatings Technology, 2002, 154(1): 14−20.
[13] CAMPOS I, OSEGUERA J, FIGUEROA U, GARCIA J A, BAUTISTA O, KELEMENIS G. Kinetic study of boron diffusion in the paste-boriding process [J]. Materials Science and Engineering A, 2003, 352(1−2): 261−265.
[14] MELENDEZ E, CAMPOS I, ROCHA E, BARRON M A. Structural and strength characterization of steels subjected to boriding thermochemical process [J]. Materials Science and Engineering A, 1997, 234−236(30): 900−903.
[15] LOU D C, SOLBERG J K, AKSELSEN O M, DAHL N. Microstructure and property investigation of paste boronized pure nickel and Nimonic 90 superalloy [J]. Materials Chemistry and Physics, 2009, 115(1): 239−244.
[16] SAHIN S, MERIC C. Investigation of the effect of boronizing on cast irons [J]. Materials Research Bulletin, 2002, 37(5): 971−979.
[17] UEDA N, MIZUKOSHI T, DEMIZU K, SONE T, IKENAGA A, KAWAMOTO M. Boriding of nickel by the powder-pack method [J]. Surface and Coatings Technology, 2000, 126(1): 25−30.
[18] OZBEK I, AKBULUT H, ZEYTIN S, BINDAL C, UCISIK A H. The characterization of borided 99.5% purity nickel [J]. Surface and Coatings Technology, 2000, 126(2−3): 166−170.
[19] EFE G C, IPEK M, OZBEK I, BINDAL C. Kinetics of borided 31CrMoV9 and 34CrAlNi7 steels [J]. Materials Characterization, 2008, 59(1): 23−31.
[20] EKMEKCILER E, POLAT A, USTA M. Hard boride coating on iron aluminide (FeAl) [J]. Surface and Coatings Technology, 2008, 202(24): 6011−6015.
[21] ATAR E, KAYALI E S, CIMENOGLU H. Characteristics and wear performance of borided Ti6Al4V alloy [J]. Surface and Coatings Technology, 2008, 202(19): 4583−4590.
[22] MIAO Zhu-jun, SHAN Ai-dang, WANG Wei, LU Jun, XU Wen-liang, SONG Hong-wei. Solidification process of conventional superalloy by confocal scanning laser microscope [J]. Transactions of Nonferrous Metals Society of China, 2011, 21(2): 236−242.

标准热处理对 718 硼化镍铬合金显微组织和性能的影响

邓德伟，王春光，刘倩倩，牛婷婷

大连理工大学 材料科学与工程学院，大连 116024

摘　要：将 718 铬镍铁合金进行渗硼处理。为了得到强度和塑性的最佳组合，对硼化 718 铬镍铁合金进行标准热处理，包括固溶处理和双级时效处理。硼化层由化合物层和硼扩散区组成。由于硼化层有较高的硬度，与没有渗硼的 718 铬镍铁合金相比，硼化 718 铬镍铁合金的磨损率显著减少，摩擦因数也较低。标准热处理可以有效促进硼扩散到材料的内部，并促进新硼化物(Fe_2B，CrB)的生成。经过标准热处理的硼化 718 铬镍铁合金由于其较厚的渗硼层(313.76 μm)而表现出较好的耐磨性。

关键词：渗硼；718 铬镍铁合金；标准热处理；耐磨性；耐腐蚀性能

(Edited by Yun-bin HE)